Article

Brain-Derived Reconstituted Lipid Nanoparticles Show Selective Homing to Ischemic Brain

Dan Han and Cheng Wang *

Posted Date: 17 July 2023

doi: 10.20944/preprints202307.1054.v1

Keywords: reconstituted lipid nanoparticles; selective homing; ischemic stroke

Article

Brain-Derived Reconstituted Lipid Nanoparticles Show Selective Homing to Ischemic Brain

Dan Han [1] and Cheng Wang [2,*]

[1] Department of Pharmacy, Nanjing Drum Tower Hospital, The Affiliated Hospital of Nanjing University Medical School, Nanjing, China
[2] School of Pharmacy, Changzhou University, Changzhou 213164 Jiangsu, China
* Corresponding author: Cheng Wang: wangc90@cczu.edu.cn.

Abstract: Lipid nanoparticles (LNPs) are promising carriers for constructing drug delivery systems (DDSs) in disease treatments. Previous studies have suggested that lipid composition and biophysical properties of LNPs can significantly impact their interaction with cells and tissues, allowing for the development of suitable LNPs for precise drug delivery. Our previous study proposed the concept and facile preparation of reconstituted lipid nanoparticles (rLNPs), which not only have the advantages of traditional LNPs but also contain the lipids of mother cell/tissue. In this study, we have found that brain-derived rLNPs (B-rLNPs) can have much better accumulation to the ischemic area of the ischemic stroke (IS) model than liver-derived rLNPs (L-rLNPs). This homing effect hopefully makes rLNPs a useful tool for developing highly accessible devices with homologous targeting ability for precise drug delivery.

Keywords: reconstituted lipid nanoparticles; selective homing; ischemic stroke

1. Introduction

Lipid nanoparticles (LNPs) represent a unique kind of drug delivery carrier that is composed of mainly physiological lipids. [1-2] It can be subdivided into many useful carriers, including solid lipid nanoparticles, nanostructured lipid carriers, and liposomes. [3] They have been widely practiced as suitable drug delivery carriers for various drugs [4-6] and in different disease models, [7-8] due to their multiples advantages, including facile large-scale production, high biocompatibility, controllable drug loading and release, convenient surface modification, etc. [9] Therefore, the development of suitable LNPs based drug delivery system (DDS) is one of the important orientations in disease treatments. [10-11] Previous studies have shown that lipid composition and biophysical properties of LNPs can significantly impact their interaction with cells and tissues, allowing for the tailored design of DDSs with specific targeting capabilities. [12-15] In this regard, it is hoped to find suitable LNPs for precise drug delivery.

In the previous study, we proposed the concept and preparation of reconstituted lipid nanoparticles (rLNPs), which can be easily applied to develop highly reproducible cell/tissue-based nanocarriers for drug delivery. [16] The rLNPs not only have the advantages of traditional LNPs but also contain the lipids of mother cell/tissue, which offers the opportunity to inhere some of the natures of mother cell/issue for potential homotypic interaction and targeted delivery. As a proof of concept, here in our study, we developed two types of rLNPs. One is prepared from the brain tissue of mouse while the other is from liver tissue. Using liver-derived rLNPs (L-rLNPs) as control, we compare the selective accumulation of these two carriers using fluorescence labeling to see if brain-derived rLNPs (B-rLNPs) can show better targeted distribution to the ischemic area of ischemic stroke (IS) model.

 doi:10.20944/preprints202307.1054.v1

2. Materials and methods

Mice and study approval

In this study, male C57BL/6 mice (11-12 weeks old, weighing 20-22 g) were purchased from the Model Animal Research Center of Nanjing University. All mice were housed with free access to diet and water under standard laboratory conditions. Block randomization was used in this study. The animal experiments were conducted in accordance with The Guidelines for Animal Care and Use of Laboratory Animals published by the National Institutes of Health and the protocol was approved by the Institutional Ethics Committee of Nanjing Drum Tower Hospital (permit number: 2020AE01037). All efforts were made to minimize the number of animals used.

Preparation of nanoparticles

All chemical reagents in the following article without specific statements were from Aladdin (Shanghai, China) and of analytical pure. The preparation of both rLNPs was in line with the previous report. [16] In brief, 50 mg brain tissue or liver tissue (from male C57BL/6 mice) was homogenized with 200 μL 75% methanol solution. The mixture then was re-homogenized with 500 μL MTBE and kept shaking for 1 h. After that, 125 μL ultra-pure water was added to the solution to promote the separation of the biphasic system. Then the solution was centrifuged at 14000 rpm, 4 ℃ for 15 min. At last, the supernatant part was collected to dry with a nitrogen blower to obtain corresponding lipid extractions. The obtained lipids were weight and again dissolved in ethanol to achieve designated concentrations. Afterward, the solvent diffusion method was applied by injecting the ethanol solution into pure water (volume ratio of 1: 9) at a constant rate via a syringe under gentle agitation to obtain corresponding rLNPs.

Proper amounts of fluorescent molecules (1,1′-dioctadecyl-3,3,3′,3′-tetramethylindocarbocyanine perchlorate (DiI or IR780) were dissolved in ethanol solution with the extracted lipids and then injected into pure water as mentioned above to prepare drug-loaded (B-rLNPs/NBP) or fluorescent molecule labeled rLNPs (L-rLNPs/DiI, B-rLNPs/DiI, L-rLNPs/IR780 and B-rLNPs/IR780). The unlabeled fluorescent molecules were removed by filtration through a 0.22 μm membrane (Millipore, USA).

Characterization of nanoparticles

The size and surface charge were measured by dynamic light scattering (Bettersize, Shanghai, China) in triplicate. The morphology was observed by transmission electron microscope (TEM, JEM-1010, JEOL, Tokyo, Japan). Besides, to evaluate their stability behavior, L-rLNPs and B-rLNPs were re-dispersed in PBS and plasma at room temperature (RT), and their particle size changes were measured at 3 h, 6 h 9 h, 12 h, 24 h, 36 h, and 48 h in triplicate.

Induction of middle cerebral artery occlusion/Reperfusion (MCAO/R)

MCAO/R model was established as IS model according to our previous study. [17] Briefly, transient cerebral ischemia was induced by MCAO with silicon suture (Guangzhou Jialing Biotech Co., Ltd, Guangzhou, China) under anesthesia with 1% isoflurane in the anesthetic mask. After 1 h of MCAO, the suture was removed for reperfusion (R). Mice in sham group were conducted by the same procedure but without arterial ligation. Mice's respiratory rate and body temperature were monitored by a physiological monitor during the surgery.

Optical imaging of rLNPs accumulation in the brain

L-rLNPs/IR780 and B-rLNPs/R780 were intravenously administered respectively to model mice (MCAO/R) at 24 h after surgery (n=3). At 72 h after MCAO/R, the *in vivo* distribution of IR780 signal at the brain of mice was recorded using In Vivo Imaging System (IVIS Spectrum, PerkinElmer, USA). The mice were then sacrificed and their brains were harvested for further *ex vivo* imaging using the same instrument. In parallel, L-rLNPs/DiI and B-rLNPs/DiI were intravenously administered

Preprints (www.preprints.org) | NOT PEER-REVIEWED | Posted: 17 July 2023 doi:10.20944/preprints202307.1054.v1

respectively to the same model mice (n=3). The infarction area was confirmed at 72 h after MCAO/R by magnetic resonance imaging (MRI) as mentioned in the following. Afterward, high-resolution distribution of rLNPs in the brain was detected by tissue fluorescent imaging. In brief, mice were anesthetized with isoflurane, then the brains were removed and frozen at -80 ℃. Coronal brain sections (10 μm) were cut on a freezing sled microtome (Thermo Scientific, USA) and widefield overview images of brain slides were obtained with THUNDER Imager 3D Assay (Leica, Germany). In addition, the same brain tissues slides were incubated with 1% 2, 3, 5-Triphenyltetrazolium chloride (TTC, Sangon Biotech Co., LTD) at 37 ℃ for 20 min for hematoxylin-eosin (H&E) staining as mentioned in the following. The infarct volume was expressed as a percentage of the volume of the contralateral hemisphere.

3. Results

Characterization of nanoparticles

As shown in Figure 1A, both rLNPs prepared from the liver and brain were nanosized particles. The Z-average size for L-rLNPs and B-rLNPs was 73.83 nm and 53.36 nm, respectively. The polydispersity index (PDI) of both rLNPs was around 0.1, indicating the well-dispersion of the as-prepared rLNPs. The zeta potential for these two types of nanoparticles was -25.61 mV and -27.61 mV, respectively. The TEM results in Figures 1B and C revealed that the morphology of both nanoparticles was near-spherical to irregular polygon while L-rLNPs were more isotropic in appearance. Both rLNPs showed good colloidal stability in PBS and plasma for more than 48 h (Figure 1D and E), indicating their high stability under the physiological environment upon *in vivo* administration.

A

Sample	Particle Size (nm)	Zeta Potential (mV)	Polydispersity Index(PDI)
L-rLNPs	73.83 (Z-average)	-25.61	0.108
B-rLNPs	53.36 (Z-average)	-27.61	0.101

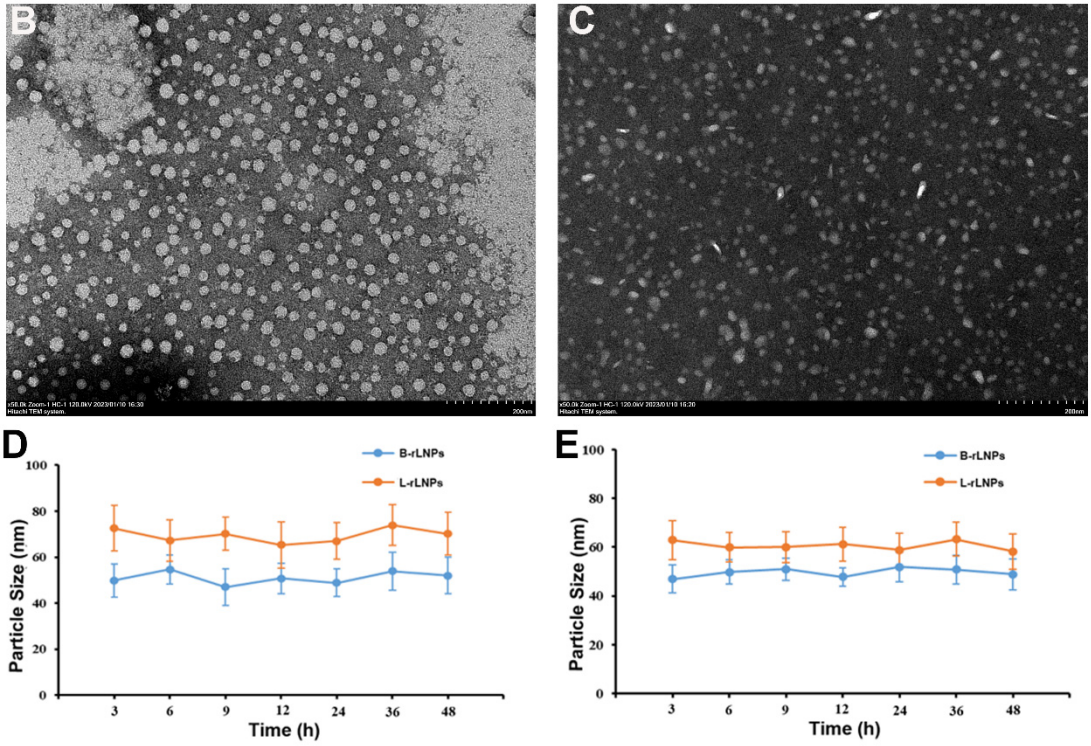

Preprints (www.preprints.org) | NOT PEER-REVIEWED | Posted: 17 July 2023 doi:10.20944/preprints202307.1054.v1

Figure 1. Characterization of nanoparticles. (A) The Z-average particle size, zeta potential, and PDI of different rLNPs. The TEM image of L-rLNPs (B) and B-rLNPs (C). The scalr bar is 200 nm. The colloidal stability of both rLNPs in (D) PBS (pH 7.4) and (E) plasma. Data were shown as mean ± S.D. n=3.

Selective IS homing of B-rLNPs

After labeling with near infrared fluorescent dye IR780, the *in vivo* brain distribution of both rLNPs was studied. As displayed in Figure 2A, at 48 h post a single intravenous injection, both rLNPs showed accumulation to the brain while the accumulation of B-rLNPs was significantly higher than that of L-rLNPs. The *ex vivo* imaging in Figure 2B also confirmed this conclusion and also revealed that both rLNPs can selectively accumulate to the IS area (right) instead of the normal one (left). In Figure 2C, using the high-resolution tissue fluorescent imaging to monitor the DiI labeled rLNPs in parallel, it was shown that the concentrated fluorescent signals were highly overlaid with the IS area (confirmed by MRI and H&E staining), which concluded that both rLNPs have targeting preference to IS area. In particular, B-rLNPs showed much higher distribution to the IS area than that of rLNPs, indicating that B-rLNPs might have a selective homing ability to IS.

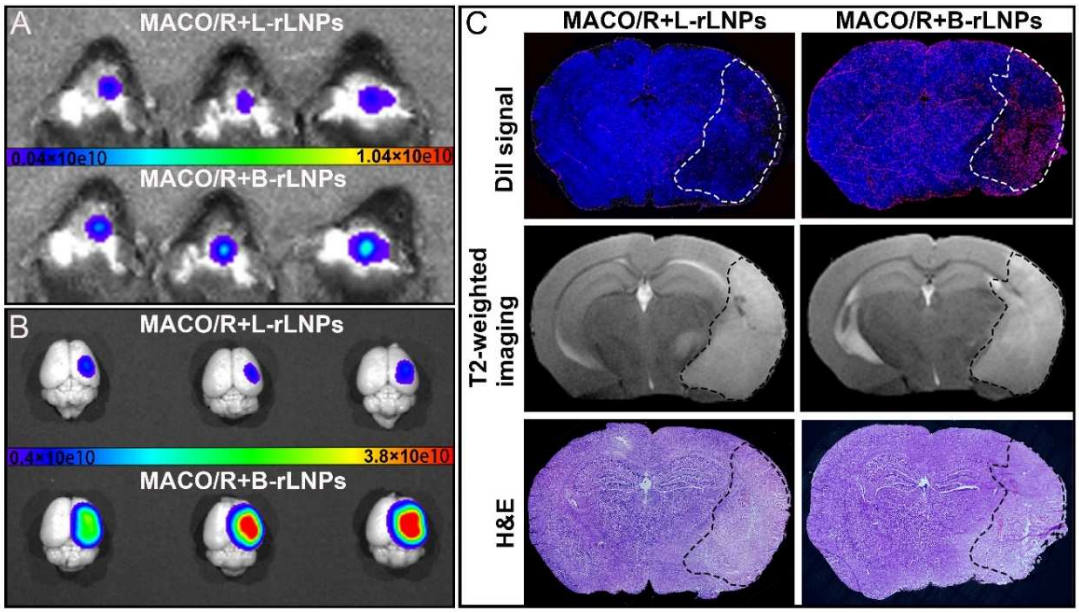

Figure 2. Selective homing of B-rLNPs into the cerebral ischemic area induced by IS. The *in vivo* (A) and *ex vivo* (B) imaging of the distribution of DiI labeled rLNPs in the brain at 72h after MCAO/R by the live imaging system. (C) Representative brain sections with accumulation of DiI labeled rLNPs in infarct area (confirmed by T2-weighted imaging and H&E staining) caused by MCAO/R.

4. Discussion

In a previous study, we introduced the concept and preparation of rLNPs as a means to develop highly reproducible carriers derived from both cells and tissues for drug delivery. [16] The rLNPs not only retain the advantages of traditional LNPs but also preserve lipids from the mother cells or tissues, thus enabling the inheritance of certain characteristics for potential homotypic interactions and targeted delivery. In this study, two nanosized rLNPs from the liver and brain of C57BL/6 mice were successfully prepared using the same method (Figure 1) and results revealed that both rLNPs showed good colloidal stability under different physiological environments (PBS and plasma) for more than 48 h (Figure 1D and E), which were beneficial for the long-circulation and continuous accumulation to the IS area. Taking advantage of the flexible labeling/modification merits of rLNPs, they were labeled with fluorescent molecules (DiI and IR780) to help demonstrate their distribution in the brain. By tracing the signal of these fluorescent molecules, it was revealed that although both rLNPs have accumulation to the IS area, B-rLNPs showed a much better homing profile to the IS than

that of L-rLNPs. From the results of Figure 1, it can conclude that both rLNPs showed good dispersion and shared similar particle size, zeta potential, and morphology, which means these physical properties might not have an important impact on their *in vivo* behavior. Therefore, it was suggested that the lipid components might be responsible for their differentiated accumulation to the IS area, and positive targeting might be involved in the process.

In our opinion, this positive targeting effect might due to two main reasons: 1) Positive transportation of B-rLNPs to the IS area by specific proteins; 2) Positive cell recognition of B-rLNPs by specific cells within IS area. Previous studies revealed the upregulation of caveolin-1-expression and activation of caveolae-mediated transcellular delivery after IS, which was responsible for the increased liposome localization to the IS area. [18-19] Therefore, in our future work, we will focus on studying whether there are differences on caveolae affinity and its mediated transportation between different originated rLNPs.

Other than the transportation, specific cell recognition can give further increased accumulation of DDSs to the lesion. A classic example is the modification of different targeting ligands to the surface of DDSs for improved drug accumulation in cancer cells. [20] In recent years, positive targeting strategies are getting increasing attention with cell-membrane vehicles as the most widely studied candidate, since cell-membrane vehicles usually inherit similar properties to the mother cells. Current researches mainly ascribe the homing effect of cell membrane-based carriers to the remaining receptors on their surface that can preserve the function of mother cells. [21] However, previous studies have also shown that lipid composition and biophysical properties of liposomes can have significant impacts on their interaction with cells. [13-14] From many aspects, cell membrane-based carriers can be considered as analogous to liposomes. Therefore, it is reasonable to suggest that lipid-based cell membrane interaction might be involved and contribute to the homing effect of cell membrane-based carriers. Moreover, LNPs with different components have been shown to afford tailored designs of DDSs with specific targeting capabilities. For instance, effective targeting of specific tissues can be accomplished by optimizing the pKa value of the LNP membrane through the incorporation of various lipids with distinct pKa values into a single formulation. [15] Furthermore, it has been proposed that the internal and/or external charge of LNPs can play a crucial role in modulating tissue tropism. Supplementing established LNP with additional molecules can tune the internal charge of LNPs, thereby influencing the cellular response *in vivo*. [12] It was therefore suggested that the specific lipid components of B-rLNPs that differ from L-rLNPs might be an important reason for their selective homing to the IS. As expected, our results in Figure 2 suggested a better homing effect of B-rLNPs than L-rLNPs, which gives primary support to this suggestion. In our future works, we will try to elucidate the underlying mechanisms.

5. Conclusion

In conclusion, in this study, with similar size, surface charge, and morphology, B-rLNPs show a better homing effect than L-rLNPs. This is an exciting result that has the potential to make rLNPs a facile and highly accessible tool to replace the traditional targeted drug delivery carriers, such as cell membrane-derived vehicles and ligand-modified carriers, for precise drug delivery, which might open up a new avenue for drug delivery and disease management.

References

1. Nakamura, T.; Sato, Y.; Yamada, Y.; Abd Elwakil, M. M.; Kimura, S.; Younis, M. A.; Harashima, H. Extrahepatic targeting of lipid nanoparticles in vivo with intracellular targeting for future nanomedicines. *Advanced Drug Delivery Reviews* **2022**, 114417.
2. Nasirizadeh, S.; Malaekeh-Nikouei, B. Solid lipid nanoparticles and nanostructured lipid carriers in oral cancer drug delivery. *Journal of Drug Delivery Science and Technology* **2020,** *55*, 101458.
3. Silva, A. C.; Moreira, J. N.; Lobo, J. M. S., Current Insights on Lipid-Based Nanosystems. MDPI: 2022; Vol. 15, p 1267.

4. Kraisit, P.; Hirun, N.; Mahadlek, J.; Limmatvapirat, S. Fluconazole-loaded solid lipid nanoparticles (SLNs) as a potential carrier for buccal drug delivery of oral candidiasis treatment using the Box-Behnken design. *Journal of Drug Delivery Science and Technology* **2021,** *63*, 102437.
5. Samaridou, E.; Heyes, J.; Lutwyche, P. Lipid nanoparticles for nucleic acid delivery: Current perspectives. *Advanced drug delivery reviews* **2020,** *154*, 37-63.
6. Dhiman, N.; Awasthi, R.; Sharma, B.; Kharkwal, H.; Kulkarni, G. T. Lipid nanoparticles as carriers for bioactive delivery. *Frontiers in chemistry* **2021,** *9*, 580118.
7. Khare, P.; Edgecomb, S. X.; Hamadani, C. M.; Tanner, E. E. L.; Manickam, D. S. Lipid nanoparticle-mediated drug delivery to the brain. *Advanced Drug Delivery Reviews* **2023**, 114861.
8. Nakamura, T.; Harashima, H. Dawn of lipid nanoparticles in lymph node targeting: Potential in cancer immunotherapy. *Advanced drug delivery reviews* **2020,** *167*, 78-88.
9. Tenchov, R.; Bird, R.; Curtze, A. E.; Zhou, Q. Lipid nanoparticles— from liposomes to mRNA vaccine delivery, a landscape of research diversity and advancement. *ACS nano* **2021,** *15* (11), 16982-17015.
10. Witzigmann, D.; Kulkarni, J. A.; Leung, J.; Chen, S.; Cullis, P. R.; van der Meel, R. Lipid nanoparticle technology for therapeutic gene regulation in the liver. *Advanced drug delivery reviews* **2020,** *159*, 344-363.
11. Zong, Y.; Lin, Y.; Wei, T.; Cheng, Q. Lipid Nanoparticle (LNP) Enables mRNA Delivery for Cancer Therapy. *Advanced Materials* **2023**, 2303261.
12. Cheng, Q.; Wei, T.; Farbiak, L.; Johnson, L. T.; Dilliard, S. A.; Siegwart, D. J. Selective organ targeting (SORT) nanoparticles for tissue-specific mRNA delivery and CRISPR–Cas gene editing. *Nature Nanotechnology* **2020,** *15* (4), 313-320, DOI: 10.1038/s41565-020-0669-6.
13. Liu, Y.; Bravo, K. M. C.; Liu, J. Targeted liposomal drug delivery: a nanoscience and biophysical perspective. *Nanoscale Horizons* **2021,** *6* (2), 78-94.
14. Peetla, C.; Stine, A.; Labhasetwar, V. Biophysical interactions with model lipid membranes: applications in drug discovery and drug delivery. *Molecular pharmaceutics* **2009,** *6* (5), 1264-1276.
15. Shobaki, N.; Sato, Y.; Harashima, H. Mixing lipids to manipulate the ionization status of lipid nanoparticles for specific tissue targeting. *International journal of nanomedicine* **2018,** *13*, 8395-8410, DOI: 10.2147/ijn.S188016.
16. Wang, C. Reconstituted Lipid Nanoparticles from Cells/Tissues for Drug Delivery in Cancer. *Molecular Pharmaceutics* **2023,** *20* (6), 2891-2898.
17. Han, D.; Fang, W.; Zhang, R.; Wei, J.; Kodithuwakku, N. D.; Sha, L.; Ma, W.; Liu, L.; Li, F.; Li, Y. Clematichinenoside protects blood brain barrier against ischemic stroke superimposed on systemic inflammatory challenges through up-regulating A20. *Brain Behav Immun* **2016,** *51*, 56-69, DOI: 10.1016/j.bbi.2015.07.025.
18. Nag, S.; Venugopalan, R.; Stewart, D. J. Increased caveolin-1 expression precedes decreased expression of occludin and claudin-5 during blood–brain barrier breakdown. *Acta neuropathologica* **2007,** *114*, 459-469.
19. Al-Ahmady, Z. S.; Jasim, D.; Ahmad, S. S.; Wong, R.; Haley, M.; Coutts, G.; Schiessl, I.; Allan, S. M.; Kostarelos, K. Selective liposomal transport through blood brain barrier disruption in ischemic stroke reveals two distinct therapeutic opportunities. *ACS nano* **2019,** *13* (11), 12470-12486.
20. Mi, P.; Cabral, H.; Kataoka, K. Ligand-installed nanocarriers toward precision therapy. *Advanced Materials* **2020,** *32* (13), 1902604.
21. He, Z.; Zhang, Y.; Feng, N. Cell membrane-coated nanosized active targeted drug delivery systems homing to tumor cells: A review. *Materials Science and Engineering: C* **2020,** *106*, 110298, DOI: https://doi.org/10.1016/j.msec.2019.110298.